

# Importance of resonance widths in low-energy scattering of weakly-bound light-mass nuclei

P. R. Fraser<sup>1,\*</sup>, K. Massen-Hane<sup>1</sup>, K. Amos<sup>2,3</sup>, I. Bray<sup>1</sup>, L. Canton<sup>4</sup>, R. Fossion<sup>5</sup>,  
A. S. Kadyrov<sup>1</sup>, S. Karataglidis<sup>3,2</sup>, J. P. Svenne<sup>6</sup>, and D. van der Knijff<sup>2</sup>

<sup>1</sup> *Department of Physics, Astronomy and Medical Radiation Sciences,  
Curtin University, GPO Box U1987, Perth 6845, Australia*

<sup>2</sup> *School of Physics, University of Melbourne, Victoria 3010, Australia*

<sup>3</sup> *Department of Physics, University of Johannesburg, P.O. Box 524, Auckland Park, 2006, South Africa*

<sup>4</sup> *Istituto Nazionale di Fisica Nucleare, Sezione di Padova, I-35131, Italy*

<sup>5</sup> *Instituto de Ciencias Nucleares, Universidad Nacional Autónoma de México, 04510, Ciudad de México, Mexico*

<sup>6</sup> *Department of Physics and Astronomy, University of Manitoba and  
Winnipeg Institute for Theoretical Physics, Winnipeg, MB, R3T 2N2, Canada*

(Dated: August 27, 2018)

What effect do particle-emitting resonances have on the scattering cross section? What physical considerations are necessary when modelling these resonances? These questions are important when theoretically describing scattering experiments with radioactive ion beams which investigate the frontiers of the table of nuclides, far from stability. Herein, a novel method is developed that describes resonant nuclear scattering from which centroids and widths in the compound nucleus are obtained when one of the interacting bodies has particle unstable resonances. The method gives cross sections without unphysical behavior that is found if simple Lorentzian forms are used to describe resonant target states. The resultant cross sections differ significantly from those obtained when the states in the coupled channel calculations are taken to have zero width, and compound-system resonances are better matched to observed values.

PACS numbers: 24.10.Eq; 24.30.-v; 25.40.Dn; 25.40.Fq; 25.60.-t

The advent of radioactive ion beams has allowed exploration of nuclei far from the valley of stability, and has led to an immense experimental effort [1–14]. Theoretical studies of these systems is vital for interpretation of the resultant data. Elastic scattering of two nuclei at low energies often gives cross sections displaying resonances associated with properties of the compound system; the analysis of which is appropriately done with a coupled-channel theory in which the low-energy spectra of the nuclei concerned are most relevant in defining the coupling interactions. Usually, however, those states are not considered to be resonances. Herein we present results found using a theory in which those target state resonance properties are taken into account. As detailed below, this requires a mathematically-robust, energy-dependent shape to avoid unphysical behaviors in calculated observables, such as vanishing bound states, irregular behavior at the scattering threshold, and with the requirement of causality being restored.

To this end, a multi-channel algebraic scattering (MCAS) method [15] is used. MCAS solves coupled-channel Lippmann-Schwinger equations in momentum space using the Hilbert-Schmidt expansion of amplitudes. In this method, two-body nuclear scattering potentials are expanded into a series of sturmians [15–17], and then a corollary between separable scattering potentials and separable  $T$ -matrices of the Lippmann-Schwinger equation delivers solutions without explicitly solving the integral equations. Scattering potentials used for this investigation treat the nuclear target as having collective rotor character [18]. However, in order to account the coupling of the incident nucleon to Pauli-forbidden orbits in the target states, one must also include an orthogonalising

pseudo-potential (OPP) [19–23], which has also been used in atomic physics [24, 25].

By solving the Lippmann-Schwinger equations in momentum space, one may describe within the same method both the bound (to particle emission) and scattering states of the compound nucleus. The bound states may be found by assuming negative projectile energies in the sturmian equations, and at the corresponding binding energies the sturmian eigenvalues are real and have a value of 1. For positive energies, to systematically identify all resonance structures we use a spectral representation of the  $S$ -matrix in terms of complex sturmian eigenvalues [16]. The trajectories of the eigenvalues in the complex-energy plane, in particular in the vicinity of the pole-position  $P(1, 0)$ , can be employed to determine each resonance centroid and width contained in the  $S$ -matrix, no matter how narrow or large the resonance may be [15].

Separable sturmian expansions of the chosen interaction potential are made using a finite ( $n$ ) set of sturmians ( $\hat{\chi}_{cn}(p)$ ); functions that are generated from the same interactions for each channel ( $c$ ), where  $c$  denotes a unique set of quantum numbers. Obtaining the sturmian eigenstates,  $\eta_p$ , requires specification of the Green's function [15]

$$[\mathbf{G}_0]_{nn'} = \mu \left[ \sum_{c=1}^{\text{open}} \int_0^\infty \hat{\chi}_{cn}(x) \frac{x^2}{k_c^2 - x^2 + i\epsilon} \hat{\chi}_{cn'}(x) dx - \sum_{c=1}^{\text{closed}} \int_0^\infty \hat{\chi}_{cn}(x) \frac{x^2}{h_c^2 + x^2} \hat{\chi}_{cn'}(x) dx \right]. \quad (1)$$

where the wave numbers are

$$k_c = \sqrt{\mu(E - \epsilon_c)} \text{ and } h_c = \sqrt{\mu(\epsilon_c - E)}, \quad (2)$$

$\epsilon_c$  is the target-state centroid and  $E$  is the projectile energy. Typically, the Green's functions are solved by methods of complex analysis.

The spectrum of the compound system is found from the resolvent in the  $T$ -matrix, namely  $[\eta - \mathbf{G}_0]^{-1}$  where  $[\eta]_{nn'} = \eta_n \delta_{nn'}$  with  $\eta_n$  being the sturmian eigenvalues. The bound states of the compound system are defined by the zeros of that matrix determinant when the energy is  $E < 0$ ; all channels then being closed.

Results using the Green's function Eq. (1) (and from those later given) are shown in Figs. 1 and 2; the first presents spectra of  ${}^9\text{Be}$  as an  $n+{}^8\text{Be}$  cluster and the second a set of total elastic and reaction cross sections in the energy range to just over 5 MeV.  ${}^8\text{Be}$  was treated as a rotor with quadrupole deformation and three states of it,  $0_{g.s.}^+$ ,  $2_1^+$  and  $4_1^+$ , used in the coupling. In Fig. 1, the spectrum for  ${}^9\text{Be}$  found using Green's functions as per Eq. (1) is shown in the column furthest right. For comparison, the experimental spectrum [26], is shown on the far left. Fig. 2 displays the cross sections found from the same calculation (and others discussed later) whose spectrum is shown in Fig. 1. The results are identified by the same notation. In this case where Eq. (1) is used, the reaction cross section only becomes non-zero above the energy of the first target state, which is at 4.81 MeV (lab frame), as necessary.

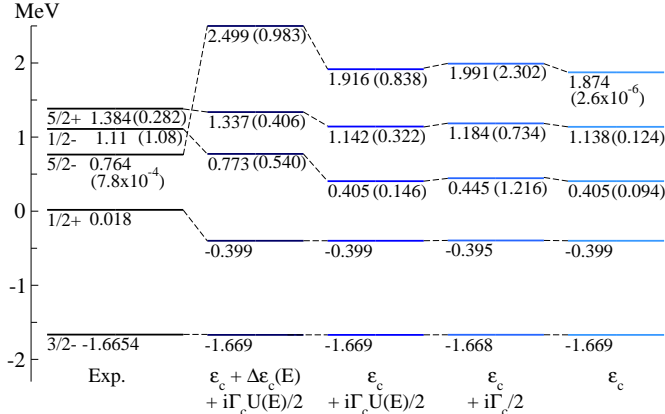


FIG. 1: (Color online.) Experimental spectrum of  ${}^9\text{Be}$  compared with MCAS calculations with target states defined as per labels (see text). Unbracketed numbers are excitation energies, bracketed numbers are widths, all in MeV.

However, in the low-energy and low-mass regime where compound-system resonances are important, it is appropriate to take particle-instability of target states into account by modifying the Green's functions. In its most basic form [27], this is done by adding a complex component to the target-state energy. That is, the description of the target state energy becomes:

$$\epsilon_c + i\frac{\Gamma_c}{2}, \quad (3)$$

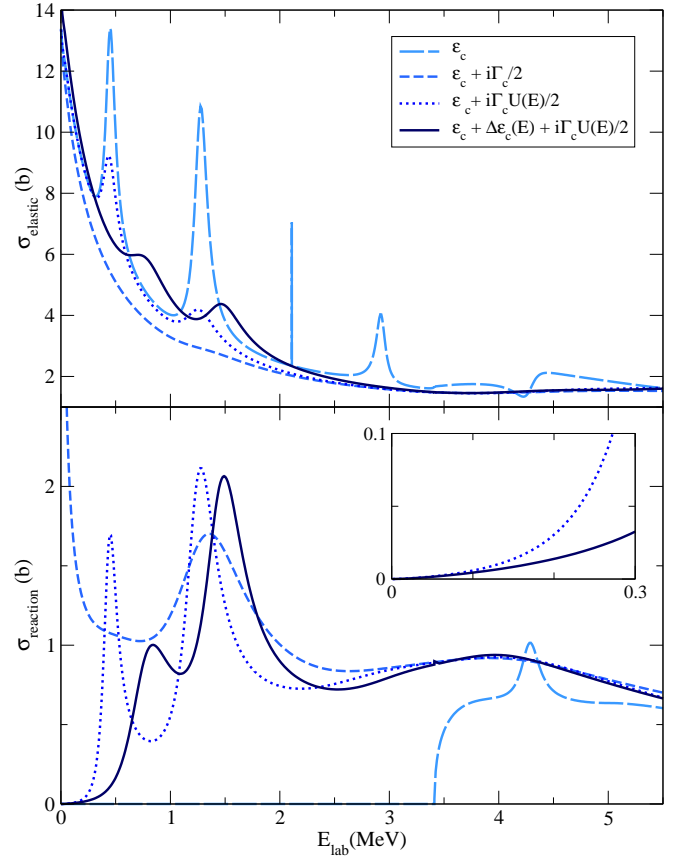


FIG. 2: (Color online.) Calculated  $n+{}^8\text{Be}$  elastic scattering (top panel) and reaction (bottom panel) cross sections. Inset shows threshold behaviour of the reaction cross sections.

and the Green's functions thus become

$$[\mathbf{G}_0]_{nn'} = \mu \left[ \sum_{c=1}^{\text{open}} \int_0^\infty \hat{\chi}_{cn}(x) \frac{x^2 \left[ k_c^2 - x^2 - \frac{i\mu\Gamma_c}{2} \right]}{[k_c^2 - x^2]^2 + \frac{\mu^2\Gamma_c^2}{4}} \hat{\chi}_{cn'}(x) dx - \sum_{c=1}^{\text{closed}} \int_0^\infty \hat{\chi}_{cn}(x) \frac{x^2 \left[ h_c^2 + x^2 + \frac{i\mu\Gamma_c}{2} \right]}{[h_c^2 + x^2]^2 + \frac{\mu^2\Gamma_c^2}{4}} \hat{\chi}_{cn'}(x) dx \right]. \quad (4)$$

This equation has no poles on the real axis, and integration may proceed normally [27]. The spectrum in Fig. 1 identified by the complex energy  $\epsilon_c + i\frac{\Gamma_c}{2}$  resulted on using the same interaction as before but with the  $2^+$  and  $4^+$  states of  ${}^8\text{Be}$  having their known particle-emission widths [26].

Cross sections are calculated using the  $S$ -matrix which has the general form:

$$S_{cc'} = \delta_{cc'} - i^{l_{c'}-l_c+1} \pi \mu \sum_{n,n'=1}^N \sqrt{k_c} \hat{\chi}_{cn}(k_c) ([\eta - \mathbf{G}_0]^{-1})_{nn'} \hat{\chi}_{c'n'}(k_{c'}) \sqrt{k_{c'}}. \quad (5)$$

where  $\eta$  is an array of sturmian eigenvalues and  $G_0$  are the same Green's function used to defined in Eq. (1) when no tar-

get state widths are considered, and Eq. (4) with states described as per Eq. (3). As the systems considered herein do not have particle emission widths in their ground states, the sturmians “in the elastic channel”  $\hat{\chi}_{1n}(k_1)$  and  $\hat{\chi}_{1n}(k_1)$  will not be different from cases where no target-state widths are considered. However,  $S$ -matrices and thus cross sections will still be altered by the inclusion of particle-emission widths through the channels of  $([\eta - \mathbf{G}_0]^{-1})_{nn'}$  not involving the target ground state. The cross sections that results from using complex energies for the  $2_1^+$  and  $4_1^+$  states in  $^8\text{Be}$ , are shown in Fig. 2, identified by the notation  $\epsilon_c + i\frac{\Gamma}{2}$ .

Of note, with particle-emission considered, the reaction cross section is non-zero from zero projectile energy upwards, due to loss of flux from target decay. However, their asymptotic behaviour at low projectile energies is unphysical, and is due to the Lorentzian form that implicitly defines the target states in Eq. (4) being non-zero at and below the scattering threshold (as also observed in a technical note, Ref. [28]). This also affects the energy of bound states, causing them to become spuriously unstable.

To overcome this non-physical behaviour, a scaling factor is applied to target-state widths, such that the target states are now described as

$$\epsilon_c + i\frac{U(E)\Gamma_c}{2}, \quad (6)$$

which changes the Green’s functions of Eq. (4) by multiplication of  $\Gamma$  in both integrals by  $U(E)$ . As minimum conditions, the scaling function  $U(E) = 0$  when  $E \leq 0$ ,  $U(E) = 1$  at energy centroid, and  $U(E) \rightarrow 0$  as  $E \rightarrow \infty$ . In addition, to fully eliminate asymptotic behaviour in the reaction cross sections as  $E \rightarrow +0$ , it is required that  $\frac{dU(E)}{dE} \rightarrow 0$  as  $E \rightarrow +0$ . See Ref. [28] for an example of where a scaling function was investigated where the last condition was not met (and where causality correction, discussed below, was not addressed.)

The concept of energy dependent widths goes back to Wigner [29], and is widely used in nuclear cross section estimates [30]. Typically, the low-energy dependence of such scaled resonances are ruled by the centrifugal (and eventually Coulomb) barrier. The probability of formation of a resonance is modulated at low energies by these “penetration” factors. It is these factors which lead to the requirement on the scaling functions that they and their derivatives are vanishing at the scattering threshold.

However, the introduction of energy-dependent widths necessitates an energy-dependent addition to the target-state centroid, transforming the energy of the state *viz.*

$$\epsilon_c + \Delta\epsilon_c(E) + i\frac{\Gamma_c U(E)}{2}. \quad (7)$$

This is because the Green’s functions define the sturmian eigenvalues of the expansion of the potential. Thus, making the prescription of the target states complex in effect makes the potential an optical potential. As detailed in Refs. [31, 32], energy-dependent complex-components in optical potentials lead to a wave equation that violates causality unless the potential is restricted by the addition of a dispersion relation

to the real part of the potential. These concepts have been used in phenomenological optical models in, for example, Refs. [33, 34].

Here, the dispersion relation is an energy-dependent adjustment of the target-state centroid energy,  $\Delta\epsilon_c(E)$ , given by

$$\Delta\epsilon_c(E) = \frac{\Gamma_c}{2} \frac{1}{\pi} P \int_0^\infty \frac{U(E')}{E' - E} dE'. \quad (8)$$

This manifests in Eq. (4) (with  $\Gamma$  multiplied by  $U(E)$ ) as wave numbers with the form

$$k_c = \sqrt{\mu(E - \epsilon_c - \Delta\epsilon_c(E))} \text{ and } h_c = \sqrt{\mu(\epsilon_c + \Delta\epsilon_c(E) - E)}. \quad (9)$$

Many nuclear targets have a ground state with no particle-emission width, and when considering the channels involving those ground states, the wave numbers have the form of Eq. (2) rather than Eq. (9), and the Green’s function of Eq. (1) applies rather than Eq. (4) (modified by  $U(E)$  and  $\Delta\epsilon_c(E)$ ).

One candidate for an energy-dependent target-state width scaling is based upon a Wigner distribution [35], modified to meet the necessary conditions:

$$U(E) = e^q \left( \frac{E}{\epsilon_c} \right)^Z e^{-q(E/\epsilon_c)^Z} H(E) \quad (10)$$

where  $q$  and  $Z$  are positive parameters. The Heaviside function ensures proper bound-state properties. The upper panel of Fig. 3 shows Eq. (10) for  $q = 1$ , and  $Z = 2$ . The lower panel shows the integrated result of Eq. (8) with  $\epsilon_c = 1$  MeV and  $\Gamma_c = 2$  MeV.

At projectile energies below that of a resonant target state’s actual centroid, the effect of reducing the width of that state increases the centroid used for purposes of defining the wave number. Conversely, at projectile energies above the actual centroid, the reduction in target state width decreases the centroid used. The transition from positive to negative centroid correction occurs at  $E < \epsilon_c$  for these values of  $q$  and  $Z$ , which is caused by the exponential suppression of the scaling function  $U(E)$  at energies larger than  $E$ . As projectile energy tends to infinity, the centroid correction tends to  $+0$ .

Column 2 of Fig. 1 shows the resonances and bound states of an MCAS calculation with resonant states defined as per Eq. (7), using the Green’s function defined accordingly, and is labelled appropriately. The calculation used the same potential as all the others, and in fact the parameters were tuned for this case. The appropriately-labelled curves in Fig. 2 show the resultant elastic and reaction cross sections. Column 3 of Fig. 1 and the matching curves of Fig. 2 show the results of the energy-dependent scaling of widths but neglecting the causality correction to the centroid energy.

It is seen from differences between columns 2 and 5 of Fig. 1 that consideration of nuclear instability in scattering calculations has non-trivial impact upon compound-state centroids, affecting how scattering potentials must be defined to match experiment. The differences between column 2 and 3 show that the causality correction accounts for a significant

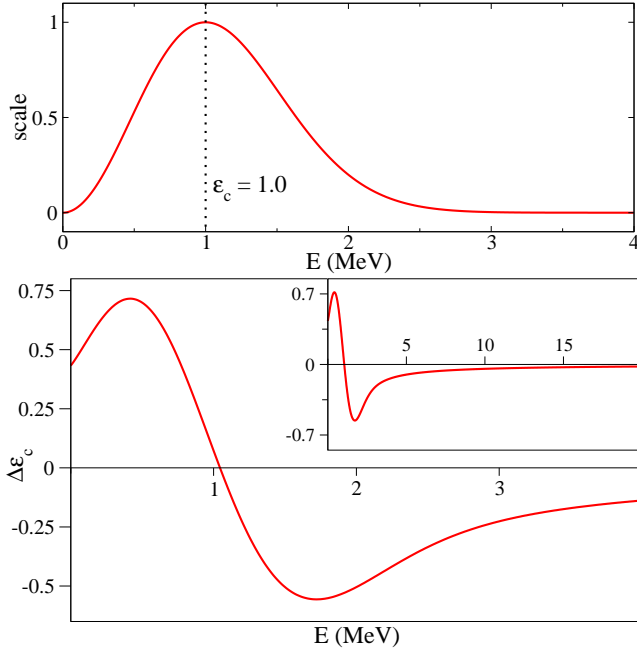


FIG. 3: (Color online.) Top: Scaling function  $U(E)$  of Eq. (10) for  $q = 1$ , and  $Z = 2$  with  $\varepsilon_c = 1$ . Bottom: Numerically evaluated  $\Delta\varepsilon_c(E)$  with  $U(E)$  having parameters as above and  $\Gamma_c = 2$  MeV. Insert shows approach to -0 as projectile energy increases.

part of this variation. The result of the full physical description of target states [column 2] gives the best centroid values for the  $\frac{1}{2}^-$  and  $\frac{5}{2}^+$  resonances, the features that dominate the calculated cross sections.

The  $\frac{1}{2}^-$  resonance is only known to decay by neutron emission, and the  $\frac{5}{2}^+$  resonance by neutron and  $\gamma$  emission [26], and so this MCAS calculation considers all important components of the resonances' widths. The calculation with no consideration of  $^8\text{Be}$  decay widths [column 5] leads a width for the  $\frac{1}{2}^-$  state that is only 9% of that observed experimentally, where the calculation with target-state width scaling and causality correction [column 2] gives a result that is 72% of the known value. The calculation in which decay widths are included but not scaled [column 4] produces 112% of the known result, but as with column 3, the calculation is unphysical as previously discussed. Regarding the  $\frac{5}{2}^+$  resonance, the width result in column 5 is 44% of the experimental value, while that of column 2 is 144%, a slightly better ratio, and that of column 4 is a large overestimation at 260%. (The centroid of the  $\frac{5}{2}^-$  resonance is poorly recreated in all calculations, and concordantly the widths are over- or under-estimated in all cases by orders of magnitude. This state is known to decay by  $\alpha$  emission, not considered here, as well as  $n$  and  $\gamma$  emission.) Thus, certainly in the case of the  $\frac{1}{2}^-$  resonance, and arguably that of the  $\frac{5}{2}^+$  resonance, consideration of particle emission from target states is seen to be a necessary ingredient in better describing scattering involving loosely-bound nuclei. Further investigation of scaling factor forms may yield yet better de-

scriptions of compound-system resonance shapes.

The appropriately-labelled curves in Fig. 2 show cross sections resulting from defining target states as per Eq. (7), and with target state width scaling but neglecting the causality correction. Again the reaction cross section is non-zero from zero projectile energy upwards due to flux loss, but it is observed that the scaling factor successfully eliminates the erroneous asymptotic rise in the reaction cross section near the threshold. This is highlighted by the inset panel. Causality restoration, by altering centroids, affects the shape of the cross sections, with consequences for scattering-potential parameterisation.

To further illustrate the effect of the Green's functions of Eq. (4) modified with  $U(E)$  and  $\Delta\varepsilon_c(E)$ , we examine a *gedanken* case of the scattering of low-energy neutrons from  $^{12}\text{C}$ , with coupling of the neutron to the  $0_1^+$ ,  $2_1^+$  and  $0_2^+$  states of  $^{12}\text{C}$ . A range of artificial particle-emission widths are assigned to the  $2_1^+$  and  $0_2^+$  states of the target, with the resulting elastic-scattering and reaction cross sections shown in Figs. 4 and 5, respectively.

Fig. 4 shows that, while the inclusion of target state widths has minimal impact upon the scattering background, with increasing target-state widths, compound-system resonances are reduced in amplitude and increased in width. With increasing target-state widths, narrow resonances are subsumed into the scattering background. The wider compound-state resonances persist to greater widths. Note that, even when not discernible from the scattering background, the method of obtaining resonances outlined above still identifies them.

The second panel of Fig. 5 shows that when target-state widths equal 0 MeV, the reaction cross section only becomes non-zero above the energy of the first target state, at 4.81 MeV (lab frame), as is necessary. When target-state widths are increased, the reaction cross section becomes non-zero for all projectile energies greater than the scattering threshold, as particle decay leads to flux loss. As target widths increase from zero, compound-system resonances immediately appear and dominate this region below the first target state energy, and then rapidly become subsumed into the scattering background. No unphysical asymptotic behavior is observed at projectile energies near the scattering threshold.

To further examine behaviour of the reaction cross section near the scattering threshold, Fig. 6 shows the case of the  $^{12}\text{C}$   $2_1^+$  and  $0_2^+$  states each having a width of 0.5 MeV with target states defined as per Eq. (3) and as defined by Eq. (7) [being a cross section of Fig. 5]. As in the  $^9\text{Be}$  investigation, the former has erroneous asymptotic behaviour as  $E \rightarrow +0$ , which is eliminated in the latter.

In conclusion, a method of accounting for states that are particle-unstable in nuclei undergoing low-energy resonant scattering is developed, which is free of unphysical behaviour at the scattering threshold and conserves causality. This is performed by choosing an appropriate target-state resonance shape, modifying a Lorentzian by use of widths dependent on projectile energy, with a correction to target-state centroid energy. Resultant scattering cross sections are markedly different from those found when particle instability is not

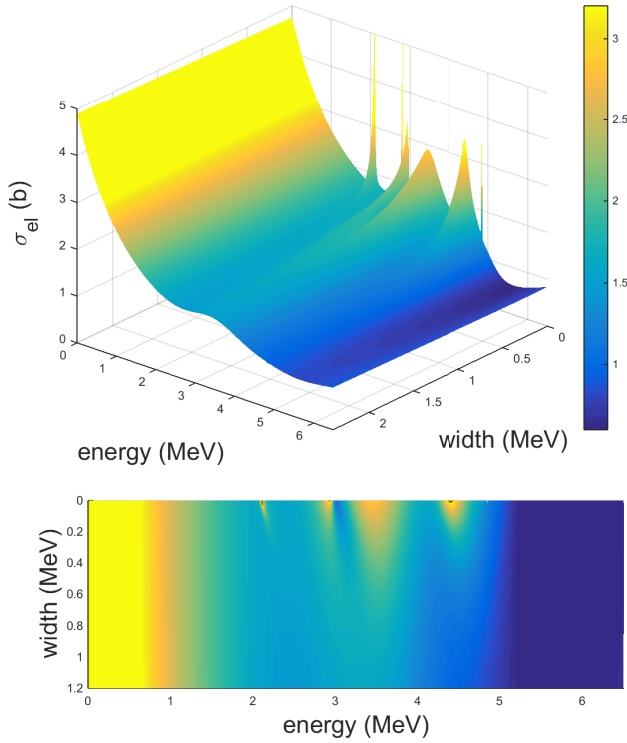


FIG. 4: (Color online.) Top:  $n+^{12}\text{C}$  elastic scattering cross section with *gedanken* particle-emission widths,  $\Gamma_c$ , of  $^{12}\text{C}$   $2_1^+$  and  $0_2^+$  states as per the axis.  $E$  is the projectile energy. Bottom: contour map detail of the top panel. Target states are as per the right of Eq. (7), with  $q = 1$ ,  $Z = 2$  in Eq. (10).

considered. Compound-system resonances decrease in magnitude and increase in width, with otherwise narrow resonances becoming obscured into the scattering background. This was shown to improve agreement between calculated and observed widths of such resonances. When using parameter-driven scattering potentials, the effects of the target-state resonance shape - and in the case energy-dependent modified Lorentzians, the centroid correction - are non-trivial in defining the potential. Compound spectra associated with, and scattering cross sections from, weakly-bound radioactive ion beams with light-mass targets should be influenced by such considerations as these.

This work is supported by the Australian Research Council, National Research Foundation of South Africa and U.S. National Science Foundation under Award No. PHY-1415656.

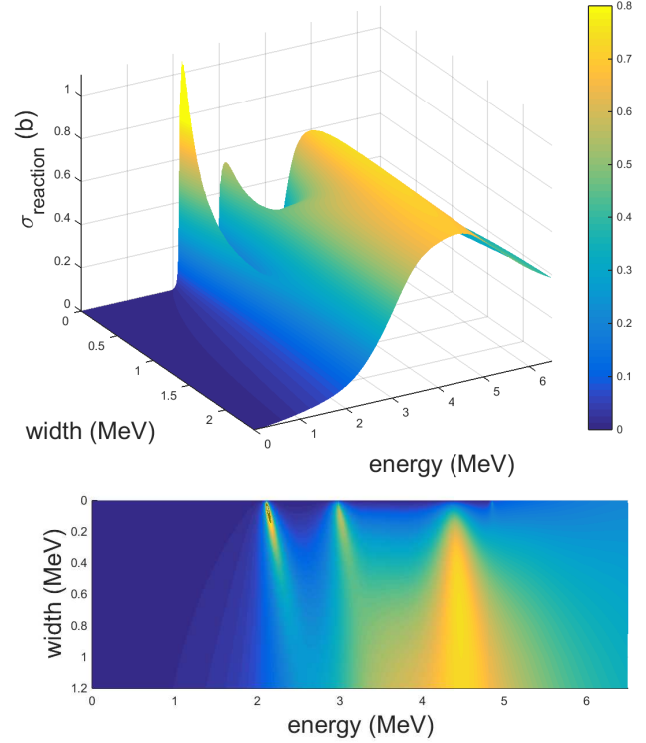


FIG. 5: (Color online.) Top:  $n+^{12}\text{C}$  reaction cross section with *gedanken* particle-emission widths,  $\Gamma_c$ , of  $^{12}\text{C}$   $2_1^+$  and  $0_2^+$  states as per the axis.  $E$  is the projectile energy. Bottom: contour map detail of the top panel. Target states are as per the right of Eq. (7), with  $q = 1$ ,  $Z = 2$  in Eq. (10).

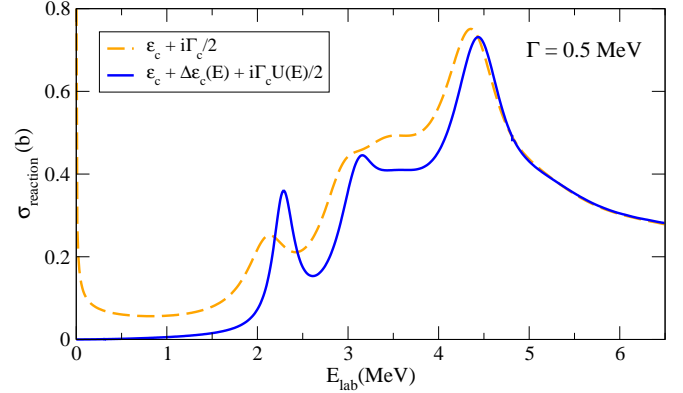


FIG. 6: Calculated  $n+^{12}\text{C}$  reaction cross for  $\Gamma_c = 0.5$  MeV.

\* Electronic address: paul.fraser@curtin.edu.au

- [1] C. A. Bertulani and G. Baur, Phys. Rep. **163**, 299 (1988).
- [2] N. Orr, J. Phys. **G38**, 020301 (2011).
- [3] M. Huyse and R. Raabe, J. Phys. **G38**, 024001 (2011).
- [4] J. R. Beene et al., J. Phys. **G38**, 024002 (2011).

- [5] G. C. Ball et al., J. Phys. **G38**, 024003 (2011).
- [6] A. Navin et al., J. Phys. **G38**, 024004 (2011).
- [7] P. V. Duppen and K. Riisager, J. Phys. **G38**, 024005 (2011).
- [8] A. B. Balantekin et al., Mod. Phys. Lett. **A29**, 1430010 (2014).
- [9] B. B. Back et al., AIP Advances **4**, 1 (2014).
- [10] F. D. Becchetti et al., Nucl. Instr. Meth. Phys. Res. **A505**, 377 (2003).
- [11] A. Lepine-Szily et al., Nucl. Phys. **A835**, 491c (2010).

- [12] H. Okuno et al., Prog. Theor. Exp. Phys. **03C002** (2012).
- [13] Z. Sun et al., Nucl. Instr. Meth. Phys. Res. **A503**, 496 (2003).
- [14] R. Rafiei et al., Nucl. Instr. Meth. Phys. Res. **A631**, 12 (2011).
- [15] K. Amos et al., Nucl. Phys. **A728**, 65 (2003).
- [16] S. Weinberg, *Lectures on Particles and Field Theory* (Prentice-Hall, Englewood Cliffs, NJ, 1965).
- [17] G. H. Rawitscher and L. Canton, Phys. Rev. C **44**, 60 (1991).
- [18] T. Tamura, Rev. Mod. Phys. **37**, 679 (1965).
- [19] V. Krasnopolsky and V. Kukulin, Soviet J. Nucl. Phys. **20**, 883 (1974).
- [20] V. Kukulin and V. Pomerantsev, Ann. of Phys. **111**, 330 (1978).
- [21] S. Saito, Prog. Theor. Phys. **41**, 705 (1969).
- [22] L. Canton et al., Phys. Rev. Lett. **94**, 122503 (2005).
- [23] K. Amos et al., Nucl. Phys. **A912**, 7 (2013).
- [24] J. Mitroy and G. G. Ryzhikh, Comp. Phys. Comm. **123**, 107 (1999).
- [25] I. A. Ivanov, M. W. J. Bromley, and J. Mitroy, Comp. Phys. Comm. **152**, 9 (2003).
- [26] D. R. Tilley et al., Nucl. Phys. **A745**, 155 (2004).
- [27] P. Fraser et al., Phys. Rev. Lett. **101**, 242501 (2008).
- [28] L. Canton et al., Phys. Rev. C **83**, 047603 (2011).
- [29] T. Teichmann and E. Wigner, Phys. Rev. p. 123 (1952).
- [30] C. Broggini, L. Canton, G. Fiorentini, and F. Villante, J. Cosmol. Astropart. Phys. **2012**, 30 (2012).
- [31] J. M. Cornwall and M. A. Ruderman, Phys. Rev. **128**, 1474 (1962).
- [32] C. Mahaux et al., Nucl. Phys. **A449**, 354 (1986).
- [33] C. Mahaux et al., Nucl. Phys. **A456**, 134 (1986).
- [34] G. Cattapan et al., Phys. Rev. C **43**, 1395 (1991).
- [35] M. Mehta, *Random Matrices* (Academic Press, NY, 1991).